

Using Big Bang Nucleosynthesis to Extend CMB Probes of Neutrino Physics

M. Shimon¹, N.J. Miller², C.T. Kishimoto³, C.J. Smith⁴, G.M. Fuller⁵ and B.G. Keating⁶

^{1,2,5,6}*Center for Astrophysics and Space Sciences, University of California, San Diego, La Jolla, CA, 92093*

³*Department of Physics and Astronomy, University of California, Los Angeles, CA, 90095*

⁴*Department of Physics, Arizona State University, Tempe, AZ, 85287*

¹*meirs@mamacass.ucsd.edu*, ²*nmiller@physics.ucsd.edu*, ³*ckishimo@physics.ucsd.edu*,

⁴*christel.smith@asu.edu*, ⁵*gfuller@ucsd.edu*, ⁶*bkeating@ucsd.edu*

ABSTRACT: We present calculations showing that upcoming Cosmic Microwave Background (CMB) experiments will have the power to improve on current constraints on neutrino masses and provide new limits on neutrino degeneracy parameters. The latter could surpass those derived from Big Bang Nucleosynthesis (BBN) and the observationally-inferred primordial helium abundance. These conclusions derive from our Monte Carlo Markov Chain (MCMC) simulations which incorporate a full BBN nuclear reaction network. This provides a self-consistent treatment of the helium abundance, the baryon number, the three individual neutrino degeneracy parameters and other cosmological parameters. Our analysis focuses on the effects of gravitational lensing on CMB constraints on neutrino rest mass and degeneracy parameter. We find for the PLANCK experiment that total (summed) neutrino mass $M_\nu > 0.29$ eV could be ruled out at 2σ or better. Likewise neutrino degeneracy parameters $\xi_{\nu_e} > 0.11$ and $|\xi_{\nu_{\mu/\tau}}| > 0.49$ could be detected or ruled out at 2σ confidence, or better. For POLARBEAR we find that the corresponding detectable values are $M_\nu > 0.75$ eV, $\xi_{\nu_e} > 0.62$, and $|\xi_{\nu_{\mu/\tau}}| > 1.1$, while for EPIC we obtain $M_\nu > 0.20$ eV, $\xi_{\nu_e} > 0.045$, and $|\xi_{\nu_{\mu/\tau}}| > 0.29$. Our forecast for EPIC demonstrates that CMB observations have the potential to set constraints on neutrino degeneracy parameters which are better than BBN-derived limits and an order of magnitude better than current WMAP-derived limits.

KEYWORDS: neutrino masses from cosmology, big bang nucleosynthesis, cosmological parameters from CMBR.

Contents

1. Introduction	1
2. Neutrinos and Neutral-Lepton Degeneracy	4
2.1 Definitions and Basic Quantities	4
2.2 Neutrino Effects on Cosmology	5
2.2.1 BBN and Light Element Abundances	6
2.2.2 The Growth of Large Scale Structure	7
3. CMB Code and Monte Carlo Simulation	10
4. M_ν and ξ_ν and Their Degeneracies with Other Parameters	11
4.1 Neutrino Mass Degeneracy	12
4.1.1 Degeneracy with w	12
4.1.2 Degeneracy with σ_8	12
4.1.3 Degeneracy with H_0	12
4.2 Neutrino Chemical Potential Degeneracy	13
4.3 Helium Fraction Degeneracy	13
5. Results	14
6. Conclusion	15

1. Introduction

The CMB is a sensitive probe of basic cosmological parameters such as the spatial curvature of the universe and the energy density in baryons, dark matter, and dark energy. Fundamental neutrino properties, such as their masses and the effective number of relativistic

degrees of freedom, are already constrained by the CMB. Forecasts for future CMB experiments, e.g. [1], indicate that neutrino properties will be constrained with unprecedented accuracy. These constraints, together with results from next-generation terrestrial experiments, may enable otherwise unobtainable insights into fundamental neutrino physics. These results will be complementary to future terrestrial experiments as well as other cosmological probes (*e.g.*, galaxy surveys [2–5], Ly α systems [6, 7], joint CMB and galaxy surveys [8–11], weak lensing [12–15] and joint CMB and weak lensing [16, 17]).

Most CMB features are imprinted at the epoch of recombination. However, post-recombination effects that introduce secondary temperature anisotropy (*e.g.*, lensing of the CMB by large scale structure (LSS) and the late integrated Sachs-Wolfe (ISW) effect) and polarization (CMB lensing by LSS) can be used to set tighter constraints on certain cosmological parameters. Although neutrinos only weakly interact, they have been present for the entire history of the universe and can leave their imprint on both the CMB and LSS. This allows high-sensitivity and high-resolution CMB experiments to probe neutrino properties through the effect of the neutrinos on LSS.

The impact of neutrinos on the CMB strongly depends on their rest masses. Solar and atmospheric neutrino oscillation experiments have shown that at least two neutrino states are massive [18]. These neutrino experiments are sensitive to the differences in the squares of the neutrino masses, but not to their absolute mass scale (solar: $\delta m_{21}^2 = 7.65_{-0.20}^{+0.23} \times 10^{-5} \text{ eV}^2$; atmospheric: $|\delta m_{31}^2| = 2.40_{-0.11}^{+0.12} \times 10^{-3} \text{ eV}^2$). In addition, these neutrino experiments have not yet determined the sign of δm_{31}^2 . If it is positive, then the neutrino mass states are in the normal hierarchy, with two lighter mass states and one heavier mass state; otherwise, if it is negative, then the neutrino mass states are in the inverted hierarchy with two heavier mass states and one lighter mass state. To pin down the three neutrino masses, a third independent measurement is required, for example, a measurement of the total, summed neutrino mass, $M_\nu \equiv \sum_{i=1,2,3} m_{\nu_i}$. Laboratory measurements of the neutrino mass-squared differences, imply that at least one neutrino mass must exceed 0.049 eV. Thus, resolving the neutrino mass hierarchy (*i.e.*, mass ordering of the solar and atmospheric mass-squared doublets) may require sensitivity to the total neutrino mass of $M_\nu < 0.1 \text{ eV}$. For $M_\nu \gtrsim 0.1 \text{ eV}$, the two mass hierarchies are indistinguishable, but if the total neutrino mass could be constrained below this level, the inverted mass hierarchy would be ruled out.

Another fundamental issue is how well cosmological probes can constrain the neutral lepton number. The lepton number residing in thermal neutrino seas can be characterized by neutrino degeneracy parameters, $\xi_i = \mu_i/k_B T_\nu$ (where μ_i is the neutrino chemical potential of the i th species (ν_e , ν_μ or ν_τ), k_B is the Boltzmann constant and T_ν is the neutrino temperature) where neutrinos have a Fermi-Dirac distribution. Current CMB data does not require the inclusion of neutrino chemical potentials in the cosmological model. In standard cosmology, the neutrino degeneracy parameters are assumed to be zero. However, there are a number of non-standard mechanisms that could lead to large neutral lepton asymmetries [19–22]. Although calculations suggest that these asymmetries may

equilibrate in the early universe [23–26], it is interesting to treat the lepton asymmetries in the three neutrino flavors independently.

Extracting neutrino masses from LSS tracers should account for the possibility that their chemical potentials do not vanish. A detection of nonvanishing neutral-lepton-asymmetry may have far-reaching implications. The current best upper limits on neutrino degeneracy parameters, which are invariant under cosmological expansion, are provided by a comparison of big bang nucleosynthesis (BBN) calculations with the observed abundance of light elements, especially ^4He [27]. Current upper limits on ξ from analysis of the CMB are of order unity, while upper limits from BBN are on the order $\xi \sim 0.1$. In this work we explore how these limits may be tightened by using future cosmological data.

This paper discusses the constraints on neutrino masses and degeneracy parameters that can be obtained from CMB data alone. In particular, we study the experimental capacity of PLANCK ¹, POLARBEAR ² and EPIC [28] to constrain these parameters. We constructed a joint BBN+CMB pipeline which self-consistently solves for the helium fraction, Y_p , given the other cosmological parameters and allows all three neutrino chemical potentials to vary independently of each other. The helium fraction is not an independent parameter in our analysis (a similar approach was adopted in [29–31]). Rather, we employ a BBN code [32–34] to self-consistently obtain Y_p from a given set of other cosmological parameters, such as Ω_b , H_0 and ξ_{ν_e} , ξ_{ν_μ} and ξ_{ν_τ} . Here the three neutrino degeneracy parameters are treated as phenomenological time-independent parameters, although models of time-dependent neutrino chemical-potentials have also been considered in the literature, e.g. [22]. Note, however, that neutrino oscillations at the solar mass-squared splitting scale can “even-up” the lepton numbers for the different neutrino flavors - a process suggested by [25] and shown to work more or less efficiently (to within a factor of ten) by [26], [23] and [24]. The ultimate effect of this oscillation-driven process would be to keep all the lepton numbers all the same and subsequently fixed with time. Y_p is an important ingredient in the physics of recombination since it determines the Silk damping scale for a fixed baryon number. Earlier works discussing the implications of precise CMB observations on helium abundance inference are, e.g. [35–37] and more recently [38]. Our analysis also benefits from CMB lensing extraction achieved by employing the standard quadratic estimators of the lensing potential [39]. This is important in exploring neutrino physics since it has been demonstrated that most of the information on neutrino parameters is encapsulated in CMB lensing [1, 40].

This work adds to previous efforts [29–31]) which have attempted to constrain the neutrino degeneracy parameters from CMB or CMB+BBN by including gravitational lensing extraction of the CMB allowing the various degeneracy parameters to vary independently. Recently, a similar analysis for WMAP5 was carried out which allowed $\xi_{\nu_e} \neq \xi_{\nu_\mu} = \xi_{\nu_\tau}$ [30]. The PLANCK, POLARBEAR, and EPIC experiments have even higher sensitivity and resolution than WMAP. This can facilitate lensing extraction, allowing them to better probe

¹<http://www.rssd.esa.int/index.php?project=planck>

²<http://bolo.berkeley.edu/polarbear/>

neutrino parameters.

The paper is organized as follows. In section 2, we discuss the effects of neutrinos on BBN and the growth of structure. Section 3 describes our Monte Carlo Markov Chain (MCMC) simulation and the modifications we introduced in CAMB. The degeneracies of neutrino mass and helium abundance with other parameters are especially relevant for parameter estimations from CMB observations and are therefore extensively discussed in section 4. We describe our results in section 5 and conclude in section 6.

2. Neutrinos and Neutral-Lepton Degeneracy

2.1 Definitions and Basic Quantities

Over the history of the universe considered in this work the distribution functions of neutrinos (ν) and anti-neutrinos ($\bar{\nu}$) with physical momentum p are

$$\begin{aligned} f_\nu(p; T_\nu, \xi) &\approx \frac{1}{e^{\frac{p}{T_\nu} - \xi} + 1} \\ f_{\bar{\nu}}(p; T_\nu, \xi) &\approx \frac{1}{e^{\frac{p}{T_\nu} + \xi} + 1}, \end{aligned} \quad (2.1)$$

where $\xi \equiv \mu/T_\nu$ is the degeneracy parameter and T_ν is the time-dependent neutrino temperature [41]. From here on, we will use natural units where $\hbar = c = k_B = 1$. The degeneracy parameter is a comoving invariant. We assume that at some point in the early universe neutrinos and anti-neutrinos were in thermal and chemical equilibrium with the photon-baryon plasma and therefore $\xi_\nu + \xi_{\bar{\nu}} = 0$. The cosmic neutrino background (CνB) temperature is inversely proportional to the cosmological scale factor, a , and is related to the (post-recombination) CMB blackbody temperature by $T_\nu = (4/11)^{1/3} T_{\text{CMB}}$.

It is convenient to write the neutrino energy density and pressure in terms of the comoving momentum, $q = pa$ [42]:

$$\begin{aligned} \rho_\nu + \rho_{\bar{\nu}} &= \frac{a^{-4}}{2\pi^2} \int_0^\infty q^2 dq \sqrt{q^2 + (aM)^2} [f_\nu(q/a; T_\nu, \xi) + f_{\bar{\nu}}(q/a; T_\nu, \xi)] \\ P_\nu + P_{\bar{\nu}} &= \frac{a^{-4}}{6\pi^2} \int_0^\infty q^2 dq \frac{q^2}{\sqrt{q^2 + (aM)^2}} [f_\nu(q/a; T_\nu, \xi) + f_{\bar{\nu}}(q/a; T_\nu, \xi)], \end{aligned} \quad (2.2)$$

where $M \equiv m_\nu/T_{\nu 0}$, with the CνB temperature at the current epoch, $T_{\nu 0} \approx 1.95$ K.

The degeneracy parameter is related to the neutral lepton number,

$$L_\nu \equiv \frac{n_\nu - n_{\bar{\nu}}}{n_\gamma} = \frac{1}{33\zeta(3)} (\pi^2 \xi + \xi^3), \quad (2.3)$$

where n_ν , $n_{\bar{\nu}}$ and n_γ are the number densities of neutrinos, anti-neutrinos and photons respectively, and $\zeta(3) \approx 1.202$ is the Riemann zeta function with argument 3.

The effective number of relativistic species, N_{eff} , is a ratio between the energy density in a given relativistic species and the energy density of the same relativistic species with a thermal distribution and zero chemical potential. If a neutrino and anti-neutrino of a given flavor both have Fermi-Dirac spectra and have equal and opposite degeneracy parameters [*e.g.*, Eq. (2.1)], then the effective number of relativistic species contributed by this neutrino flavor is

$$N_{\text{eff}} = 1 + \frac{30}{7} \left(\frac{\xi}{\pi}\right)^2 + \frac{15}{7} \left(\frac{\xi}{\pi}\right)^4. \quad (2.4)$$

The change in the total effective number of relativistic species is often used to describe the effects of non-standard neutrino distributions. When different degeneracy parameters are introduced for each neutrino flavor, the change in the overall effective number of relativistic species is

$$\Delta N_{\text{eff}} = \sum_i \left[\frac{30}{7} \left(\frac{\xi_i}{\pi}\right)^2 + \frac{15}{7} \left(\frac{\xi_i}{\pi}\right)^4 \right]. \quad (2.5)$$

ΔN_{eff} is a useful parameter when the detectable effects of neutrinos on the CMB depend on the contribution of these particles to the energy density in radiation. However, upcoming CMB experiments will have the sensitivity to probe effects that are dependent on the distribution of neutrino energies. In addition, BBN abundances are sensitive to neutrino energy distributions. Hence, ξ_ν will be more useful than ΔN_{eff} in the analysis of upcoming CMB experiments.

2.2 Neutrino Effects on Cosmology

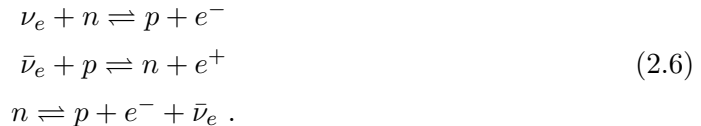
Neutrinos have a wide range of effects on the evolution of the universe. In the early universe they participate in the reactions that determine the neutron-to-proton ratio which, in turn, affects the abundances of the light elements produced during BBN. Later, at a redshift of $z \approx 3200$, the energy density in the ν B helps determine the epoch of matter-radiation equality. At recombination, $z \approx 1100$, the universe was not purely matter dominated, implying that gravitational potential wells had decayed, slightly. This leads to the early ISW effect, which boosts the CMB temperature anisotropy angular power spectrum on multipole scales associated with the horizon scale, $l \lesssim 200$. Neutrinos play a role in this process because the fraction of the total energy density in the form of radiation (which is sensitive to neutrino masses and degeneracy parameters, Eq. 2.2) determines the amplitude of the ISW effect. This is the only effect of neutrino mass and degeneracy parameter that can be probed by WMAP and other moderate angular resolution experiments. Fig. 1 shows the calculated CMB power spectrum for various ξ , along with the data points from WMAP5. It is clear that $\xi > 1$ is excluded at 1σ (assuming all other parameters are fixed). A global parameter analysis reaches a similar conclusion [30].

An aspect highlighted in this paper is that stringent constraints on neutrino mass and degeneracy parameters can come from an analysis of CMB lensing. A neutrino that is non-relativistic today could have been relativistic at higher redshifts. Non-relativistic

neutrinos could be captured into potential wells, while relativistic neutrinos would act as hot dark matter (HDM) and would freely stream, resulting in an apparent suppression of structure formation during the epochs when the neutrinos are relativistic. Precise measurements of the LSS power spectrum can be used to place constraints on neutrino masses and degeneracy parameters.

2.2.1 BBN and Light Element Abundances

BBN occurs at temperatures much higher than the current upper bounds on neutrino masses and therefore BBN calculations cannot constrain neutrino masses. However, the neutrino degeneracy parameters impact BBN abundance-yields by affecting both the reaction rates that determine the neutron-to-proton ratio and the expansion-rate of the universe, which helps to determine how neutron-to-proton inter-conversion works. The weak reactions that set the neutron-to-proton ratio are



The rates of these reactions depend on the number density and energy spectrum of ν_e and $\bar{\nu}_e$, which in turn depend on the electron neutrino degeneracy parameter, ξ_{ν_e} [27, 43–46]. These reaction rates compete with the expansion rate of the universe which is determined by the total energy density; the latter also depends on all neutrino degeneracy parameters, Eq. (2.2). It is clear, therefore, that BBN distinguishes ξ_{ν_e} from ξ_{ν_μ} and ξ_{ν_τ} , making for a nontrivial interplay between the neutrino degeneracy parameters and the light element abundances, particularly ${}^4\text{He}$.

Combined analysis of the CMB (BOOMERANG and DASI experiments), BBN (helium and deuterium abundance) and SNIa data yield the following 2σ limits [47]

$$\begin{aligned}
 -0.01 &< \xi_{\nu_e} < 0.22 \\
 |\xi_{\nu_\mu, \nu_\tau}| &< 2.6.
 \end{aligned}
 \tag{2.7}$$

If oscillation between the three neutrino species results in equilibration of the asymmetries among the neutrino flavors [23–25], then the more stringent ${}^4\text{He}$ constraint on ξ_{ν_e} applies to all neutrino flavors and BBN considerations suggest [27, 45, 48]

$$|\xi_\nu| \lesssim 0.1.
 \tag{2.8}$$

However, non-standard physics could lead to different degeneracy parameters for the three different neutrino flavors.

BBN determines the abundance of light elements, including the helium fraction, Y_p . These abundances can be sensitive to the baryon closure fraction, Ω_b , and the three neutrino

degeneracy parameters. In particular, Y_p is determined principally by the neutron-to-proton ratio at temperatures $T \sim 100$ keV. This ratio is set by the competition between the weak reactions in Eq. (2.6). As a result, Y_p depends strongly on the neutrino degeneracy parameters.

Until recently, the helium fraction was usually considered as a free parameter in CMB analyses. Recent work [29–31] has attempted to self-consistently include Y_p as a non-independent parameter in CMB power spectra calculations. It was noted in [31] that certain cosmological parameters are significantly biased when Y_p is fixed at $Y_p = 0.24$ and consistency with BBN is ignored.

Helium recombination occurs prior to hydrogen recombination. Therefore, for a fixed baryon closure fraction, the number density of free electrons at hydrogen recombination is a function of the helium abundance. The Silk damping scale is the scale over which temperature anisotropy and polarization will be washed out by free-streaming of photons between the onset and the end of decoupling. This scale depends on the photon mean free path which is inversely proportional to the number density of free electrons. Increasing Y_p reduces the number density of free electrons at hydrogen recombination, which increases the mean free path of the CMB photons. The result would be a suppression of correlations on larger angular scales, which would shift Silk damping to lower multipole numbers.

2.2.2 The Growth of Large Scale Structure

While weak constraints on neutrino masses can be extracted from the primary CMB power spectra, adding probes of structure formation has the potential to significantly tighten these bounds. Using CMB lensing rather than resorting to other cosmological probes of structure formation is nearly systematic-free, providing high fidelity constraints.

CMB lensing is a sensitive probe of any cosmological parameter that impacts the growth rate of gravitational potential wells. Current CMB data, combined with observational data from Type Ia Supernovae (SNIa) and baryon acoustic oscillations (BAO), constrains the total neutrino mass to the sub-eV level [49]. Since the lensed CMB is the result of the integrated effect of the lensing of the primary CMB by structure formation, and the relevant redshift range for structure formation may overlap with the epoch where neutrinos transition from being relativistic to non-relativistic, the CMB can be a powerful tracer of neutrino masses and degeneracy parameters. Additional leverage on neutrino free streaming comes from e.g., galaxy correlations, Ly α forest power spectra [3, 50] and weak galaxy lensing [16].

Tracers of the matter power spectrum, such as CMB lensing, are sensitive to the epoch when neutrino momenta were redshifted to a point where they are non-relativistic. This is because non-relativistic neutrinos behave as a cold dark matter (CDM) and contribute to the growth of structure, while relativistic neutrinos behave as HDM and suppress structure on scales below their free streaming scale. Thus, the epoch when neutrinos become

non-relativistic is important in discerning the effect of neutrinos on large scale structure. Both the neutrino mass and degeneracy parameter determine when neutrinos become non-relativistic.

Probes of the growth of structure in the universe indicate that CDM, rather than HDM, is the dominant component of matter. Neutrino masses of $0.2 - 0.3$ eV (consistent with the upper limits in the current neutrino mass constraints) are mildly relativistic at recombination which would result in the slight decay of gravitational potential wells at last scattering, leading to a primary ISW effect. For a spatially flat universe, $\Omega_k = 0$, and a fixed dark energy density fraction, Ω_Λ , changing the neutrino masses will change the amount of HDM at a given redshift at the expense of CDM. This will cause a relative suppression of structure formation at high redshifts. In turn, this will be reflected in the level of CMB lensing by LSS. Several forecasts for PLANCK, CMBPOL³ and other CMB experiments suggest that constraints on neutrino masses can be improved by a factor of three to four [1], provided the experiments have sufficiently high sensitivity and angular resolution to allow lensing extraction. As already mentioned, the CMB, galaxy redshift surveys, cluster abundances, Ly α and other sensitive probes of the growth of structure on scales of a few tens of Mpc can be employed to set sub-eV constraints on the total neutrino mass. An intriguing question is whether these probes could distinguish between the normal and inverted neutrino mass hierarchies. Constraining the total neutrino mass below the required ~ 0.1 eV scale is a challenging task in the presence of astrophysical foregrounds and other systematics. It was recently shown, e.g. [3,15], that by combining several cosmological probes, this (or similar) limit can be achieved. However, it is important to be mindful of the assumptions that are made in achieving these limits and to what extent the systematics can be controlled.

The free streaming scale can be estimated as the proper distance traveled by a neutrino over the age of the universe. This gives an estimate of the neutrino free streaming scale, λ_{FS} . This scale is

$$\lambda_{\text{FS}} = \left\langle \int_0^{t_0} v(t) \frac{dt}{a(t)} \right\rangle, \quad (2.9)$$

where $v(t)$ is the neutrino velocity, which decreases as the universe expands, $a(t)$ is the scale factor, $\langle \dots \rangle$ denotes an average with respect to the neutrino energy distribution function, Eq. (2.1), and t_0 is the time today. Matter overdensity on scales smaller than λ_{FS} will be suppressed by neutrino free streaming. This suppression factor will be proportional to Ω_ν , the neutrino energy density in closure density units.

The average free streaming scale for a neutrino species with mass m_ν and degeneracy parameter ξ is

$$\lambda_{\text{FS}}(\xi, M) = \frac{1}{F_2(\xi)} \int_{q=0}^{\infty} \int_{t=0}^{t_0} \frac{q^2}{e^{q-\xi} + 1} \frac{q dq}{\sqrt{q^2 + [a(t)M]^2}} \frac{dt}{a(t)} \quad (2.10)$$

³<http://cmbpol.uchicago.edu/>

where $M = m_\nu/T_{\nu 0}$ and $F_2(\xi)$ is the Fermi integral of order two,

$$F_2(\xi) \equiv \int_0^\infty \frac{q^2 dq}{e^{q-\xi} + 1}. \quad (2.11)$$

The free streaming scale dependence on neutrino masses and degeneracy parameter is illustrated in Figure 2. Note that the free streaming scale increases with decreasing mass and increasing degeneracy parameter. Care should be taken when simultaneously discussing neutrino degeneracy parameters (which are related to flavor states) and neutrino masses (which are related to mass states) [41].

Figure 3 illustrates how neutrino mass and degeneracy parameters affect the transfer function. The transfer function represents the effect of all physical processes that cause the primordial power spectrum to evolve into the matter power spectrum at latter epochs. The relation between the power spectrum $P_m(k; z)$ and the transfer function $T(k; z)$ can be written as

$$P_m(k; z) = A_s k^{n_s} T^2(k; z), \quad (2.12)$$

where n_s and A_s are the tilt and normalization of the primordial power spectrum. The suppression of the matter power spectrum on scales smaller than the neutrino free streaming scale is related to observable quantities. This could be obtained from galaxy surveys or inferred from the CMB angular power spectrum by deconvolving the lensing power spectrum. The change in the matter power spectrum resulting from neutrino free streaming is [51]

$$\frac{\Delta P_m(k)}{P_m(k)} \approx -8 \frac{\Omega_\nu}{\Omega_m}. \quad (2.13)$$

Here, $P_m(k) \equiv P_m(k; z = 0)$. The effect of non-vanishing neutrino mass is shown on the left side of Figure 3. As the neutrino mass increases, the free streaming scale decreases, leading to suppression of the transfer function at larger wavenumbers (note that all curves are normalized to the case of $m_\nu = 0$ at low k). The suppression of the transfer function at these large wavenumbers is more pronounced for larger neutrino masses because in this case neutrinos constitute a larger fraction of the dark matter. The effect of non-zero neutrino degeneracy parameter is shown on the right side of Figure 3. As the degeneracy parameter increases, the free streaming scale increases, leading to suppression of the transfer function at progressively smaller wavenumbers.

Figure 4 illustrates the effect of non-zero degeneracy parameters on the CMB temperature, polarization, and deflection angle power spectra (the latter is essentially a measure of the rms lensing deflection angle of the LSS, relevant to CMB lensing). The most significant differences are at large multipoles, to which current CMB experiments are blind, but PLANCK, POLARBEAR and EPIC will be sensitive. Although degeneracy parameters $\xi_\nu = 3$ are already ruled out by BBN and CMB data, we show these cases for illustrative purposes. From the plots of C_l^{TT} and C_l^{EE} we can see the effect of neutrino degeneracy parameters on scales from the acoustic horizon at recombination down to Silk damping scales. The power spectrum C_l^{dd} for lensing deflection angle, d , is suppressed in the presence of nonvanishing ξ_ν at high l . This reflects the relative suppression in the transfer

function at large wavenumbers. This effect, leads to suppression of the lensing-induced B-mode polarization that results from E-B conversion via CMB lensing by LSS. Therefore, the presence of a large ξ_ν can be constrained with high sensitivity CMB experiments which are capable of discerning small variations in the weak B-mode polarization.

3. CMB Code and Monte Carlo Simulation

As in [29, 31, 42], we modified the Boltzmann code CAMB [52] by replacing the neutrino distribution function (here $q \equiv p/T$)

$$f_\nu(q) = \frac{1}{e^q + 1} \quad (3.1)$$

with

$$f_\nu(q; \xi) = \frac{1}{2} \left(\frac{1}{e^{q+\xi} + 1} + \frac{1}{e^{q-\xi} + 1} \right) \quad (3.2)$$

everywhere, including in the expressions for energy density and pressure, as well as in the Liouville equation for neutrino density perturbations. We allowed the individual neutrino flavors to have three different degeneracy parameters ξ_{ν_e} , ξ_{ν_μ} and ξ_{ν_τ} .

Neutrino masses are subject to experimental constraints from terrestrial neutrino experiments. The neutrino masses and the degeneracy parameters are degenerate with various other cosmological parameters, presenting a challenge in attempting to determine these parameters using the CMB. For a given value of Ω_ν , both m_ν and ξ_ν are degenerate; for a fixed Ω_ν , increasing ξ_ν must be compensated by decreasing neutrino masses. To avoid this degeneracy in interpretation of our simulation results we consider m_1 , m_2 , m_3 , ξ_{ν_e} , ξ_{ν_μ} and ξ_{ν_τ} as our basic parameters (in addition to the standard cosmological parameters). The three neutrino masses are constrained by the measured mass squared differences. In this work, we used conservative gaussian priors for these differences: $\delta m_{21}^2 = 8.0 \pm 0.6 \times 10^{-5} \text{ eV}^2$ and $\delta m_{31}^2 = 2.4 \pm 0.6 \times 10^{-3} \text{ eV}^2$, which are consistent with the experimental values. In practice, these and projected future laboratory improvements in neutrino mass-squared uncertainties, have little effect on our analysis. The dominant uncertainties come from CMB data uncertainties.

CMB data is encapsulated in the angular power spectra down to scales determined by the angular resolution of the specific experiment and its instrumental noise level as compared to the CMB signal. The instrumental noise N_l in measuring the angular power spectrum for multipole l , for the autocorrelation of the temperature and polarization of the E- and B-modes are related for bolometric radiometers by $2N_l^{TT} = N_l^{EE} = N_l^{BB}$. The instrumental noise is uncorrelated between T , E , and B and increases exponentially with multipole number,

$$N_{l,\nu}^{ab} = \delta_{ab} (\theta_a \Delta_a)^2 \exp[l(l+1)\theta_a^2/8 \ln 2], \quad (3.3)$$

where a and b are either T , E , or B . Here, the noise at the frequency band centered at ν is a function of the corresponding beamwidth, θ_a , and the noise per pixel in equivalent temperature units, Δ_a . To obtain the effective noise power contributed by all frequency bands in the experiment one adds them as if they were uncorrelated gaussians

$$N_l^{aa} = \left[\sum_{\nu} (N_{l,\nu}^{aa})^{-1} \right]^{-1}. \quad (3.4)$$

We simulated parameter extraction from PLANCK, POLARBEAR and EPIC. The sensitivity and resolution we considered for these experiments are given in Table 1. The CMB power spectra C^{TT} , C^{TE} , C^{EE} and C^{BB} , together with the power spectrum of the deflection angle C^{dd} , and its cross-correlation with the temperature anisotropy, C^{Td} are calculated by CAMB for a given fiducial cosmological model. When the C_l^{Td} power spectra are calculated with the parameter **accuracy_level=1**, there are very large oscillations at $l \approx 200$. These go away when the accuracy level is increased. In order to fix this in our simulation, the C_l^{Td} at $l > 200$ in the simulated data are replaced with values calculated when setting **accuracy_level=5** in CAMB. When calculating the likelihood in CAMB, the proposed C_l^{Td} are set to the same value as the “experimental” C_l^{Td} . We found that doing so does not affect the parameter uncertainties extracted from the MCMC simulation. All power spectra are assumed gaussian and are taken to be unlensed following the conclusion of [1]. The noise in lensing reconstruction, N_l^{dd} , is a function of the observed power spectra (all four lensed \tilde{C}_l with instrumental noise, Eq.(3.3), included) and the unlensed power spectra [40] (without lensing, as obtained from CAMB for a fiducial cosmological model). In calculating N_l^{dd} we employ the publically available code [53] which makes use of the quadratic estimators [39].

4. M_ν and ξ_ν and Their Degeneracies with Other Parameters

Neutrino masses and chemical potentials are both degenerate with each other and with other cosmological parameters. We now discuss the main degeneracies of neutrino parameters with other cosmological parameters. In particular, we discuss the degeneracy of neutrino masses in section 4.1 and chemical potential in section 4.2.

In Figures 5 - 11, we examine the degeneracies between different cosmological parameters and parameters that are affected by neutrino physics, in particular M_ν , ξ_ν and Y_p . In these figures, we assume the normal mass hierarchy with $m_1 = 0.01$ eV, which corresponds to $M_\nu = 0.073$ eV when the priors on the neutrino mass squared differences mentioned in the previous section are imposed, and $\xi_\nu = 0$ when calculating the theoretically expected CMB power spectra. All other cosmological parameters are set to the best fit values of WMAP [49]. As a result, these figures illustrate the possible constraints that could be placed on the neutrino parameters if the actual values of these parameters are too small to create an effect on the CMB that could be discernible in the upcoming CMB experiments. One important point to keep in mind is that the neutrino mass-squared differences measured in the laboratory excludes any $M_\nu \lesssim 0.058$ eV.

4.1 Neutrino Mass Degeneracy

Cosmological probes of neutrino masses are sensitive to the kinematics of individual neutrinos. Since the gravitational interaction is flavor-blind, it does not distinguish between neutrino species. However, for a fixed total mass it does depend on how this mass is distributed between the three species [42].

4.1.1 Degeneracy with w

As mentioned above, the suppression of the matter power spectrum in the presence of massless neutrinos on scales much smaller than the neutrino free-streaming scale is $\Delta P_m(k)/P_m(k) \approx -8\Omega_\nu/\Omega_m$. Thus, increasing Ω_ν as a result of increasing the neutrino mass can be compensated by increasing Ω_m . However, to keep the universe spatially flat, the closure fraction of the dark energy must be lowered – this is achieved by forcing the dark energy equation of state parameter, w , to be more negative. Therefore, increasing m_ν is degenerate with lowering w as illustrated in Figure 5. One way to avoid this degeneracy is to ignore cosmological information from scales smaller than the neutrino damping scale (which comes at the cost of significantly weakening the power of the CMB as a diagnostic tool of neutrino properties). Another possibility to avoid the $M_\nu - w$ degeneracy is to employ supplementary measures of distance, e.g., BAO or SNIa [49].

4.1.2 Degeneracy with σ_8

The fluctuation in the matter density on $8h^{-1}$ Mpc scales is

$$\sigma_8 = \frac{1}{2\pi^2} \int P_m(k)W(kR)k^2 dk, \quad (4.1)$$

where $W(kR)$ is a window function, $h = H_0/(100 \text{ km/s/Mpc})$, and $R = 8h^{-1}$ Mpc. Therefore, σ_8 is a function of both A_s and n_s , the normalization and tilt of the power spectrum, respectively. It is also a function of neutrino masses and degeneracy parameters, as well as any other cosmological parameters which may affect structure formation and the evolution of LSS on scales smaller than a few Mpc (Eq. 2.12). Since σ_8 represents the mass fluctuation on ~ 10 Mpc scales, and is therefore subject to neutrino free-streaming we can expect a slight $M_\nu - \sigma_8$ degeneracy, at least for CMB experiments which are sensitive to angular scales that correspond to neutrino free streaming scales. However, this degeneracy is very weak in practice as can be seen from Figure 6; no such degeneracy is expected to be observed in the PLANCK data.

4.1.3 Degeneracy with H_0

Previous studies have shown an anti-correlation between neutrino mass and the Hubble constant. The anti-correlation results from the fact that while all three neutrino mass

states are at least mildly-relativistic at recombination (consistent with the WMAP constraints on neutrino mass [49]), at least two of these mass states are non-relativistic today (consistent with the δm^2 values from neutrino experiments). As a consequence, the neutrinos contribute to Ω_m today, but contributed to Ω_r (the closure fraction in radiation energy density) at recombination. Since neutrinos with larger rest masses will constitute a larger fraction of the CDM at the current epoch, larger neutrino masses imply a larger Ω_r , relative to Ω_m , on the surface of last scattering which, in turn, gives an enhanced ISW effect. Most of the extra power due to this effect is on scales somewhat larger than the horizon (the first acoustic peak), effectively extending the first acoustic peak to larger scales. This effect can be mimicked by lowering H_0 , because a lower H_0 implies a larger horizon at decoupling.

Figure 7 shows the degeneracies between M_ν and H_0 for PLANCK, POLARBEAR, and EPIC. In these plots, the $M_\nu - H_0$ degeneracy described above is not evident. This results from the fact that these high resolution experiments will constrain neutrino masses primarily from lensing information, instead of through the ISW effect at low multipoles. For these high resolution experiments, the neutrino free streaming length is the more relevant quantity that relates to observables. This is an example of how the higher resolution and sensitivities of upcoming CMB experiments open windows to new effects that may lift parameter degeneracies.

4.2 Neutrino Chemical Potential Degeneracy

Including nonzero neutrino degeneracy parameters in the analysis introduces new parameter degeneracies. In Figure 8, the degeneracy between ξ_ν and M_ν is shown. A naive interpretation is that for a given neutrino free streaming length, increasing ξ_ν must be compensated by increasing the neutrino mass. However, the range of allowed neutrino masses and chemical potentials does not allow such a parameter degeneracy in the neutrino free streaming scale (see also Fig. 2). The mild degeneracy shown here comes from the physics at recombination through the decay of potential wells and the ISW effect. Nonvanishing neutrino degeneracy parameters increase the energy density in neutrinos for fixed neutrino masses. Increasing the neutrino energy density must be compensated by increasing the density of CDM in order to keep $\Delta P_m/P_m \approx -8\Omega_\nu/\Omega_m$ unchanged. This degeneracy can be seen in Figure 9.

4.3 Helium Fraction Degeneracy

The helium fraction affects the physics of recombination primarily by changing the Silk damping scale. The baryon closure fraction, Ω_b , is obtained to high precision from the amplitudes of the acoustic peaks of the CMB. For a given Ω_b , more helium implies less hydrogen and fewer free electrons on the surface of last scattering. This causes a larger photon mean free path, which damps CMB temperature anisotropy on larger angular scales. This effect can be mimicked by either reducing the normalization of the primordial power spectrum or increasing its tilt. Both the $Y_p - A_s$ and the $Y_p - n_s$ planes are shown in

Figure 10. There is a significant difference in the Y_p axes between the $\xi_\nu = 0$ and the $\xi_\nu \neq 0$ cases; BBN data and the current precision on cosmological parameters tightly constrain Y_p , but allowing ξ_ν to be nonzero affects the BBN-calculated yield for Y_p and allows these degeneracies to manifest themselves in the analysis. The dilution of the free electron density at the epoch of last scattering also can be compensated by increasing $\Omega_b h^2$ as can be seen in Figure 11.

5. Results

We adopt a 14 parameter cosmological model with priors on neutrino masses taken from neutrino oscillation data. Our model is consistent with the concordance cosmological model [49]. With this model, a BBN+CMB MCMC analysis demonstrates that PLANCK and POLARBEAR will be able to measure a total neutrino mass of 0.29 eV (PLANCK) and 0.75 eV (POLARBEAR) at the 95% confidence level. In addition, neutrino degeneracy parameters can be constrained to be smaller than 0.11 (ξ_e) and 0.49 (ξ_μ, ξ_τ) for PLANCK and 0.62 (ξ_e) and 1.1 (ξ_μ, ξ_τ) for POLARBEAR. The former constraint on ξ_{ν_e} is already better than the corresponding BBN one, Eq. (2.7).

It is interesting to examine the sensitivities of upcoming CMB experiments to the neutral lepton asymmetries. If the neutrino asymmetries equilibrated through neutrino oscillations prior to the BBN epoch, then the possible constraints on the neutrino degeneracy parameters become very strong, $\xi_{\nu_e} = \xi_{\nu_\mu} = \xi_{\nu_\tau} < 0.06$ [54].

Our analysis with the extended parameter space yields weaker constraints on neutrino masses. For example, in the minimal model (all ξ_ν are set to 0) the PLANCK 2σ upper limit on M_ν is 0.27 eV. When the degeneracy parameters are turned on, the corresponding upper limit on M_ν rises to 0.29 eV. The 1σ confidence range on the electron neutrino degeneracy parameters are $-0.0314 < \xi_{\nu_e} < 0.108$ for PLANCK and $-0.017 < \xi_{\nu_e} < 0.33$ for POLARBEAR. The reason for the skewness of the distribution towards positive ξ_{ν_e} values results from the fact that ν_e determines the reaction rates of the processes described in Eq. (2.6) and also the expansion rate. In contradistinction, ξ_{ν_μ} and ξ_{ν_τ} affect only the expansion rate.

Perhaps the ultimate CMB experiment to address B-mode related issues is the mission concept, EPIC. We find that EPIC will be able to set an upper limit on the total neutrino mass of ~ 0.20 eV at 2σ confidence. In addition, we find that EPIC data alone will have sufficient sensitivity to constrain the neutrino degeneracy parameters to a level which can compete with the current constraints on degeneracy parameters derived from the primordial abundance of light elements. We derive the following limits on the degeneracy parameters: $\xi_{\nu_e} < 0.045$ and $\xi_{\nu_{\mu,\tau}} < 0.29$ at 2σ . These are better than current BBN constraints, even if equilibration of the degeneracy parameters is assumed. These results are achievable without resorting to assumptions about flavor mixing in the early universe. EPIC is capable of such an improvement in sensitivity to the degeneracy parameters because of its very high

sensitivity and angular resolution which allow for the precise measurement of the B-mode polarization required for lensing extraction of the CMB.

Finally, a cautionary note on the efficacy of our analysis. It is reasonable to ask whether future CMB data will indeed warrant considering a 13- or 14-parameter model. This question is reasonable even in the context of idealized analysis presented here because CMB data is at least limited by cosmic variance and instrumental noise. In the real world it will also be limited by astrophysical foregrounds as well as systematics. As in [55], adding cosmological parameters is in general expected to improve the fit of data to the theoretical model. Defining a generalized χ^2 such as $\tilde{\chi}^2 = -2 \ln(L) + 2p$ (where L is a likelihood and p is the number of cosmological parameters in a given model) and exploring if it improves is a useful test for such models [55]. However, this requires real data, i.e. sky-maps in the CMB case. Our analysis employed a mock power spectrum which in principle we could use to generate multiple sky realizations, each one yielding a different numerical value of $\tilde{\chi}^2$. One can then statistically determine what fraction of these actually improve when we extend the model from 11 to 13 or 14 parameters. However, this procedure is time consuming and may not be necessary at this point. When the real CMB data considered in this work is available it will be straightforward to determine whether or not our generalized model gives a better fit to the data.

6. Conclusion

Within a decade the CMB has transformed from being a cosmological probe of the basic cosmological parameters to a probe of physics beyond the standard model. CMB experiments have set interesting limits on the energy scale of inflation as well as on exotic physics such as topological defects from phase transitions in the early universe and cosmological birefringence. Also, important constraints on neutrino masses have already been obtained. Although WMAP has constrained neutrino masses to the sub-eV level, it is an exciting possibility that precise CMB measurements could place stringent constraints on neutrino masses and neutral lepton asymmetries. Although the $C\nu B$ neutrinos cannot be directly detected, they can be indirectly detected through their dynamics (through their effect on the expansion rate) and kinematics (via the damping of LSS by neutrino free streaming). A convincing detection of the $C\nu B$ would be a monumental discovery in the history of cosmology.

In this paper we explored the effects of neutrino mass and nonzero neutrino degeneracy parameters on the CMB. Changing ξ_ν leads to a different value of Y_p from BBN, and Y_p affects the density of free electrons at recombination. Y_p was calculated self-consistently in our analysis by a BBN code with a given set of cosmological and neutrino parameters. No priors on Y_p were included or used in the analysis.

Our analysis is conservative in that it allows the three neutrino degeneracy parameters to be independent parameters in the analysis. Typically, the neutrino degeneracy

parameters are assumed to be equal to each other, which would be expected if the neutrino asymmetries equilibrated in the early universe. Other works have at least set $\xi_{\nu\mu} = \xi_{\nu\tau}$, since the physics of the early universe is insensitive to the difference between these parameters. However, neutrino free streaming lengths are sensitive to the absolute value of each neutrino degeneracy parameter, so we treated each degeneracy parameter independently. While the addition of data from other cosmological probes of distance scales or LSS could be included to break parameter degeneracies, we did not include them so that we could isolate the probative powers of the CMB alone.

Upcoming CMB experiments such as PLANCK, POLARBEAR, and perhaps also EPIC will have the capability to either detect the neutrino masses and degeneracy parameters or place much more stringent bounds on these parameters as compared to current constraints from WMAP. These breakthroughs in the power of the CMB to detect neutrino parameters is the direct result of the improved resolution and sensitivity of upcoming CMB experiments, allowing CMB lensing extraction to provide an ultra-sensitive handle on neutrino masses and degeneracy parameters.

Acknowledgments

We thank the referee for very helpful comments. Eric Linder is acknowledged for his useful suggestions. We acknowledge the use of the publically available code by Lesgourgues, Perotto, Pastor & Piat for the calculation of the noise in lensing reconstruction. We also acknowledge using CAMB for power spectra calculations. CK gratefully acknowledges support from DOE grant DE-FG03-91ER40662 and NASA ATFP grant NNX08AL48G. BK gratefully acknowledges support from NSF PECASE Award AST-0548262. GMF, CS and CK acknowledge partial support from NSF grant PHY-06-52626 at UCSD.

References

- [1] J. Lesgourgues, L. Perotto, S. Pastor and M. Piat, *Phys. Rev. D* **73**, 045021 (2006), [astro-ph/0511735].
- [2] W. Hu, D. J. Eisenstein and M. Tegmark, *Phys. Rev. Lett.* **80**, 5255 (1998), [astro-ph/9712057].
- [3] U. Seljak, A. Slosar and P. McDonald, *J. Cosmol. Astropart. Phys.* **0610**, 14 (2006), [astro-ph/0604335].
- [4] C. J. MacTavish *et al.*, *Astrophys. J.* **647**, 799 (2006), [astro-ph/0507503].
- [5] M. Tegmark *et al.*, *Phys. Rev. D* **74**, 123507 (2006), [astro-ph/0608632].
- [6] R. A. C. Croft, W. Hu and R. Davé, *Phys. Rev. Lett.* **83**, 1092 (1999), [astro-ph/9903335].
- [7] S. Gratton, A. Lewis and G. Efstathiou, *Phys. Rev. D* **77**, 083507 (2008), [arXiv:0705.3100].
- [8] M. Tegmark *et al.*, *Phys. Rev. D* **69**, 103501 (2004), [astro-ph/0310723].

- [9] S. Hannestad, J. Cosmol. Astropart. Phys. **0305**, 4 (2003), [astro-ph/0303076].
- [10] Ø. Elgarøy and O. Lahav, J. Cosmol. Astropart. Phys. **0304**, 4 (2003), [astro-ph/0303089].
- [11] F. De Bernardis, P. Serra, A. Cooray and A. Melchiorri, Phys. Rev. D **78**, 083535 (2008), [arXiv:0809.1095].
- [12] A. R. Cooray, Astron. Astrophys. **348**, 31 (1999), [astro-ph/9904246].
- [13] K. N. Abazajian and S. Dodelson, Phys. Rev. Lett. **91**, 041301 (2003), [astro-ph/0212216].
- [14] S. Hannestad, H. Tu and Y. Y. Y. Wong, J. Cosmol. Astropart. Phys. **0606**, 25 (2006), [astro-ph/0603019].
- [15] T. D. Kitching, A. F. Heavens, L. Verde, P. Serra and A. Melchiorri, Phys. Rev. D **77**, 103008 (2008), [arXiv:0801.4565].
- [16] K. Ichiki, M. Takada and T. Takahashi, Phys. Rev. D **79**, 023520 (2009), [arXiv:0810.4921].
- [17] I. Tereno *et al.*, Astron. Astrophys. **500**, 657 (2009), [arXiv:0810.0555].
- [18] T. Schwetz, M. Tórtola and J. W. F. Valle, New J. Phys. **10**, 113011 (2008), [arXiv:0808.2016].
- [19] X. Shi, Phys. Rev. D **54**, 2753 (1996), [astro-ph/9602135].
- [20] A. Casas, W. Y. Cheng and G. Gelmini, Nucl. Phys. B **538**, 297 (1999), [hep-ph/9709289].
- [21] M. Kawasaki, F. Takahashi and M. Yamaguchi, Phys. Rev. D **66**, 043516 (2002), [hep-ph/0205101].
- [22] M. Yamaguchi, Phys. Rev. D **68**, 063507 (2003), [hep-ph/0211163].
- [23] A. D. Dolgov *et al.*, Nucl. Phys. B **632**, 363 (2002), [hep-ph/0201287].
- [24] Y. Y. Y. Wong, Phys. Rev. D **66**, 025015 (2002) [arXiv:hep-ph/0203180].
- [25] M. J. Savage, R. A. Malaney and G. M. Fuller, Astrophys. J. **368**, 1 (1991).
- [26] K. N. Abazajian, J. F. Beacom and N. F. Bell, Phys. Rev. D **66**, 013008 (2002), [astro-ph/0203442].
- [27] J. P. Kneller, R. J. Scherrer, G. Steigman and T. P. Walker, Phys. Rev. D **64**, 123506 (2001), [astro-ph/0101386].
- [28] J. Bock *et al.*, arXiv:0906.1188.
- [29] L. A. Popa and A. Vasile, J. Cosmol. Astropart. Phys. **0806**, 28 (2008), [arXiv:0804.2971].
- [30] M. Shiraishi *et al.*, J. Cosmol. Astropart. Phys. **0907**, 005 (2009), [arXiv:0904.4396].
- [31] J. Hamann, J. Lesgourgues and G. Mangano, J. Cosmol. Astropart. Phys. **0803**, 4 (2008), [arXiv:0712.2826].
- [32] R. V. Wagoner, Ann. Rev. Astron. Astrophys. **7**, 553 (1969).
- [33] R. V. Wagoner, Astrophys. J. **179**, 343 (1973).
- [34] L. Kawano, NASA STI/Recon Technical Report N **92**, 25163 (1992).
- [35] Trotta, R., & Hansen, S. H., Phys. Rev. D **69**, 023509 (2004), [astro-ph/0306588]
- [36] Ichikawa, K., & Takahashi, Phys. Rev. D **73**, 063528 (2006), [astro-ph/0601099]

- [37] Ichikawa, K., Sekiguchi, T., & Takahashi, Phys. Rev. D **78**, 043509 (2008), [arXiv:0712.4327]
- [38] Komatsu, E., et al. 2010, arXiv:1001.4538
- [39] W. Hu and T. Okamoto, ApJ, **574**, 566 (2202) [astro-ph/0111606]
- [40] M. Kaplinghat, L. Knox and Y.-S. Song, Phys. Rev. Lett. **91**, 241301 (2003), [astro-ph/0303344].
- [41] G. M. Fuller and C. T. Kishimoto, Phys. Rev. Lett. **102**, 201303 (2009), [arXiv:0811.4370].
- [42] J. Lesgourgues and S. Pastor, Phys. Rev. D **60**, 103521 (1999), [hep-ph/9904411].
- [43] R. V. Wagoner, W. A. Fowler and F. Hoyle, Astrophys. J. **148**, 3 (1967).
- [44] C. J. Smith, G. M. Fuller and M. S. Smith, Phys. Rev. D **79**, 105001 (2009), [arXiv:0812.1253].
- [45] K. Abazajian, N. F. Bell, G. M. Fuller and Y. Y. Y. Wong, Phys. Rev. D **72**, 063004 (2005), [astro-ph/0410175].
- [46] C. J. Smith, G. M. Fuller, C. T. Kishimoto and K. N. Abazajian, Phys. Rev. D **74**, 085008 (2006), [astro-ph/0608377].
- [47] S. H. Hansen, G. Mangano, A. Melchiorri, G. Miele and O. Pisanti, Phys. Rev. D **65**, 023511 (2001), [astro-ph/0105385].
- [48] V. Barger, J. P. Kneller, P. Langacker, D. Marfatia and G. Steigman, Physics Letters B, **569**, 123 (2003), [hep-ph/0306061].
- [49] E. Komatsu *et al.*, Astrophys. J. Suppl. **180**, 330 (2009), [arXiv:0803.0547].
- [50] A. Goobar, S. Hannestad, E. Mortsell and H. Tu, J. Cosmol. Astropart. Phys. **0606**, 19 (2006), [astro-ph/0602155].
- [51] Hu, W., Eisenstein, D. J., and Tegmark, M., Phys. Rev. Lett., **80**, 5255 (1998), [astro-ph/9712057]
- [52] A. Lewis, A. Challinor and A. Lasenby, astro-ph/9911177.
- [53] L. Perotto, J. Lesgourgues, S. Hannestad, H. Tu and Y. Y. Y. Wong, J. Cosmol. Astropart. Phys. **0610**, 13 (2006), [astro-ph/0606227].
- [54] Serpico, P. D., & Raffelt, G. G., PRD, **71**, 127301 (2005), [astro-ph/0506162]
- [55] Liddle, A. R. 2004, MNRAS, **351**, L49 (2004), [astro-ph/0401198]

Experiment	f_{sky}	ν [GHz]	θ_b [1']	Δ_T [μK]	Δ_E [μK]
PLANCK	0.65	30	33	4.4	6.2
		44	23	6.5	9.2
		70	14	9.8	13.9
		100	9.5	6.8	10.9
		143	7.1	6.0	11.4
		217	5.0	13.1	26.7
		353	5.0	40.1	81.2
		545	5.0	401	∞
857	5.0	18300	∞		
POLARBEAR	0.03	90	6.7	1.1	1.6
		150	4.0	1.7	2.4
		220	2.7	8.0	11.3
EPIC	0.65	30	28	0.5	0.7
		45	19	0.3	0.4
		70	12	0.2	0.3
		100	8.4	0.2	0.3
		150	5.6	0.3	0.4
		220	3.8	0.7	0.9
		340	2.5	2.2	3.2
		500	1.7	9.4	13.3
850	1.0	740	1047		

Table 1: Sensitivity parameters of the CMB experiments considered in this work: f_{sky} is the observed fraction of the sky, ν is the center frequency of the channels in GHz, θ_b is the full width at half maximum in arc-minutes, Δ_T is the temperature sensitivity per pixel in μK and $\Delta_E = \Delta_B$ is the polarization sensitivity.

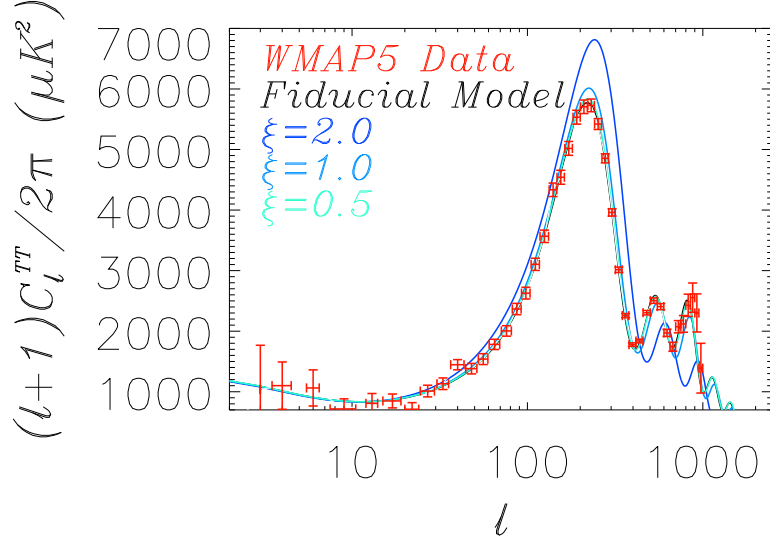


Figure 1: The calculated CMB temperature anisotropy power spectrum for $\xi_\nu = 0$ (fiducial model), 0.5, 1.0, and 2.0. The WMAP5 data points are included for reference.

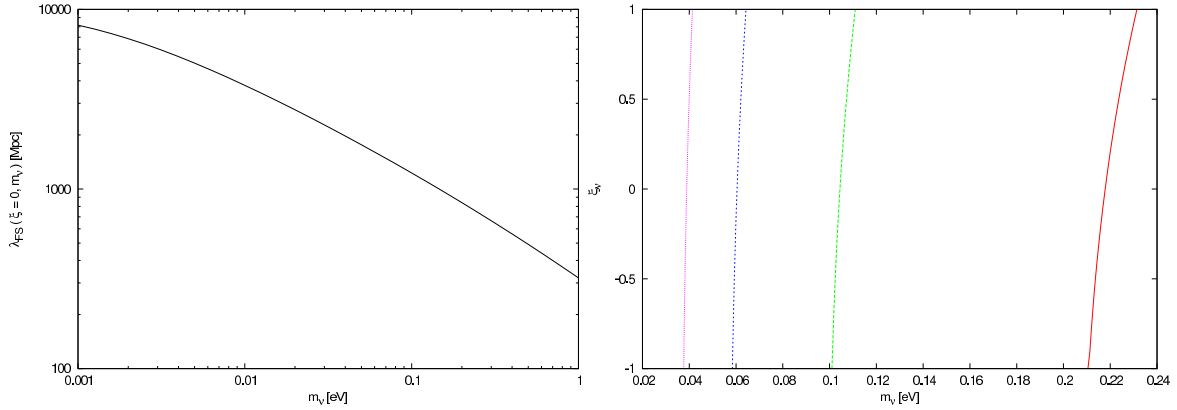


Figure 2: Neutrino free streaming scale: The figure on the left is the neutrino free streaming scale as a function of neutrino mass with $\xi_\nu = 0$. The figure on the right is a contour plot of constant free streaming scale in the m_ν - ξ_ν plane; the contours from right to left correspond to $\lambda_{FS} = 0.8, 1.2, 1.6,$ and 2.0 Gpc/h.

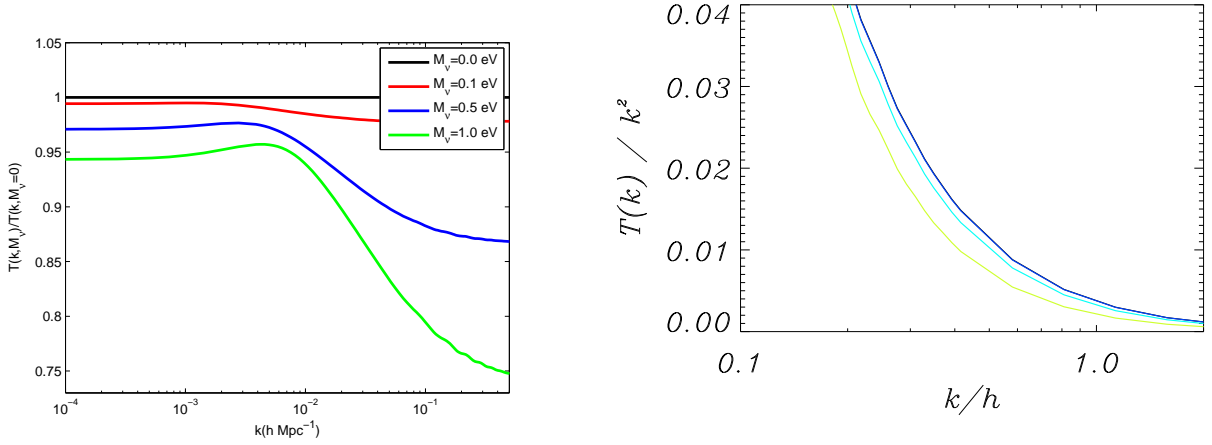


Figure 3: Susceptibility of the transfer function to M_ν (left) and ξ_ν (right). The values used for ξ are 0.1 (blue), 0.5 (cyan) and 1.0 (yellow).

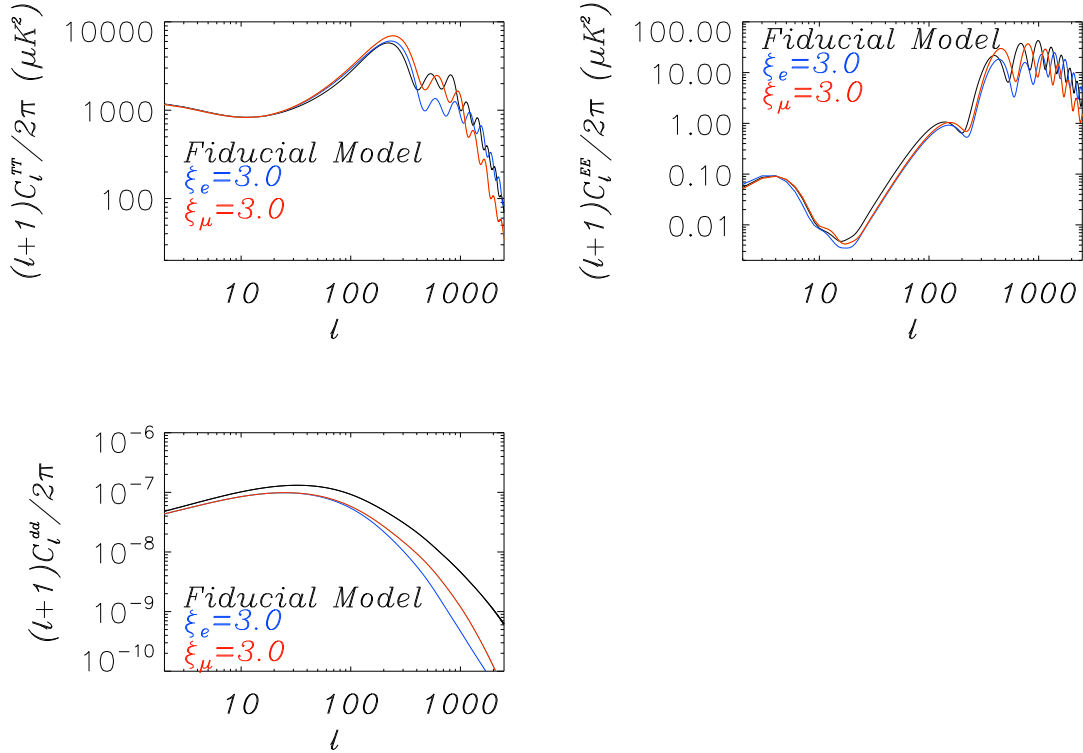


Figure 4: CMB power spectra response to changing ξ_ν : C_l^{TT} (top-left), C_l^{EE} (top-right), C_l^{dd} (bottom). In all three plots the black curves correspond to the fiducial model ($\xi_{\nu_e} = \xi_{\nu_\mu} = \xi_{\nu_\tau} = 0$), the red curves correspond to a non-zero ξ_{ν_e} model ($\xi_{\nu_e} = 3$, $\xi_{\nu_\mu} = \xi_{\nu_\tau} = 0$), and the blue curves correspond to a non-zero $\xi_{\nu_{\mu,\tau}}$ model ($\xi_{\nu_e} = 0$, $\xi_{\nu_\mu} = \xi_{\nu_\tau} = 3$).

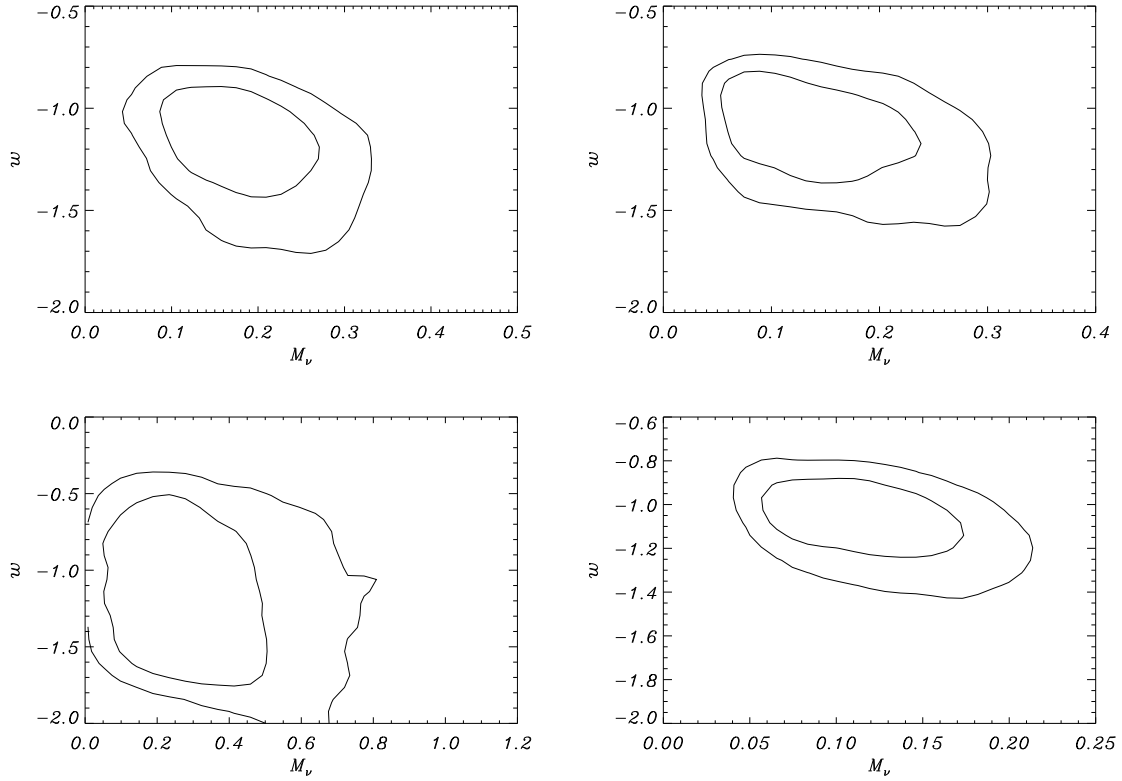


Figure 5: The M_ν - w degeneracy: Shown are the results from PLANCK $\xi_\nu = 0$ (top left), $\xi_\nu \neq 0$ (top right), POLARBEAR $\xi_\nu \neq 0$ (bottom left) and EPIC $\xi_\nu \neq 0$ (bottom right) simulations. In this plot and each successive plot, the contours correspond to the 1- and 2- σ regions. . The fiducial cosmological model is WMAP best-fit data and the neutrino masses m_2 and m_3 subject to neutrino oscillation results with m_1 assumed 0.01eV.

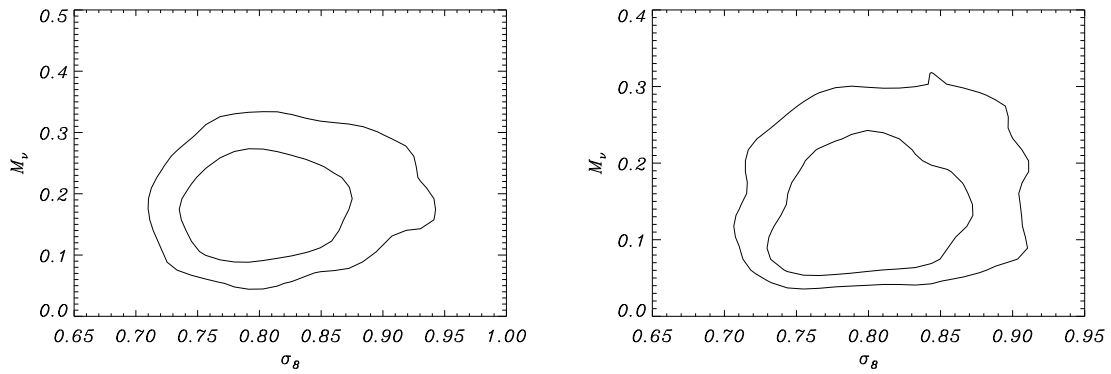


Figure 6: The M_ν - σ_8 degeneracy: Shown are the results for PLANCK in the case $\xi_\nu = 0$ (left) and $\xi_\nu \neq 0$ (right). The fiducial cosmological model is as described in Fig. 5.

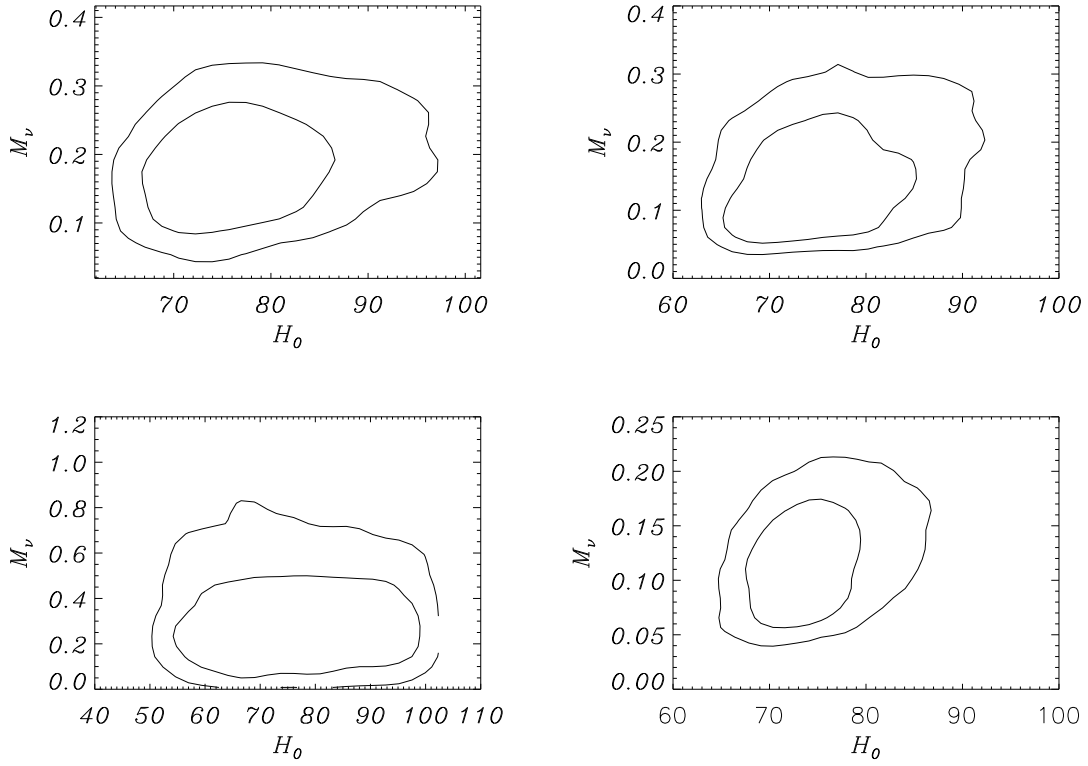


Figure 7: The M_ν - H_0 degeneracy: Shown are PLANCK ($\xi = 0$ and $\xi \neq 0$ cases on the top-left and top-right, respectively), POLARBEAR (left bottom) and EPIC (right bottom) results. For POLARBEAR and EPIC we show the generalized cosmological model with $\xi_\nu \neq 0$. The fiducial cosmological model is as described in Fig. 5.

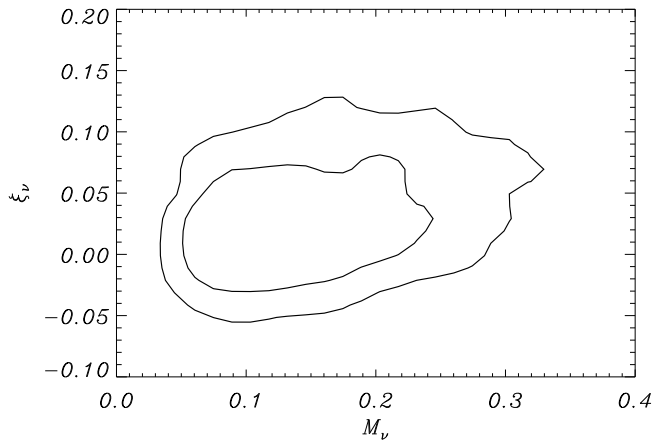


Figure 8: The M_ν - ξ_ν degeneracy for PLANCK: The fiducial cosmological model is as described in Fig. 5.

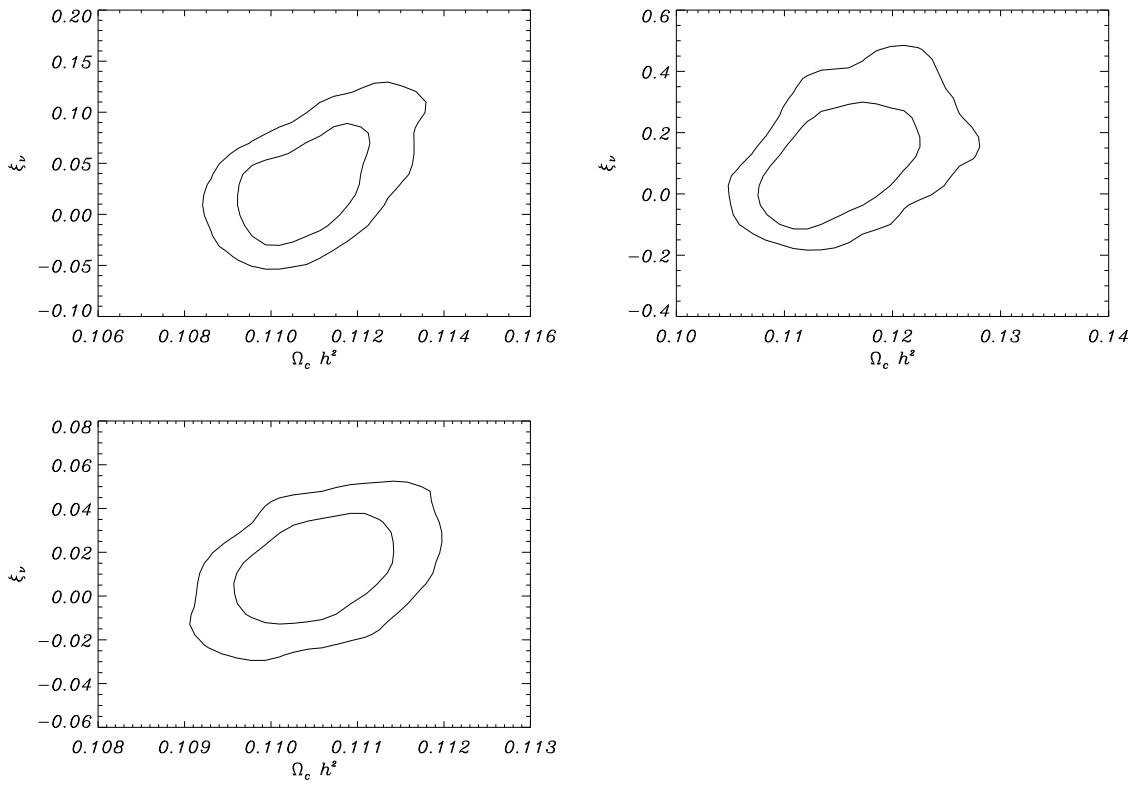


Figure 9: The $\xi_\nu - \Omega_c h^2$ degeneracy: Shown are results for PLANCK (top left), POLARBEAR (top right) and EPIC (bottom). The fiducial cosmological model is as described in Fig. 5.

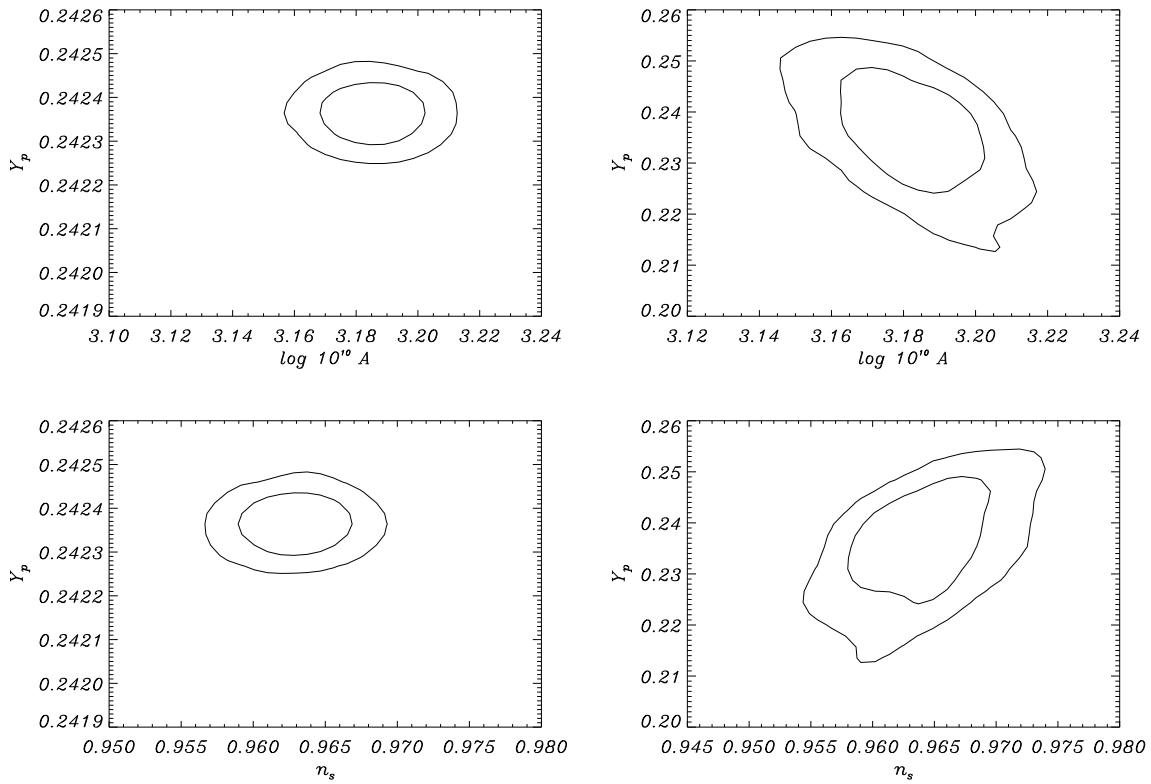


Figure 10: The degeneracy of Y_p with the normalization and tilt of the primordial power spectrum. The results for PLANCK with $\xi_\nu = 0$ are on the left and with $\xi_\nu \neq 0$ are on the right. The top two plots depict the Y_p - A_s degeneracy and bottom plots show the Y_p - n_s degeneracy. The fiducial cosmological model is as described in Fig. 5.

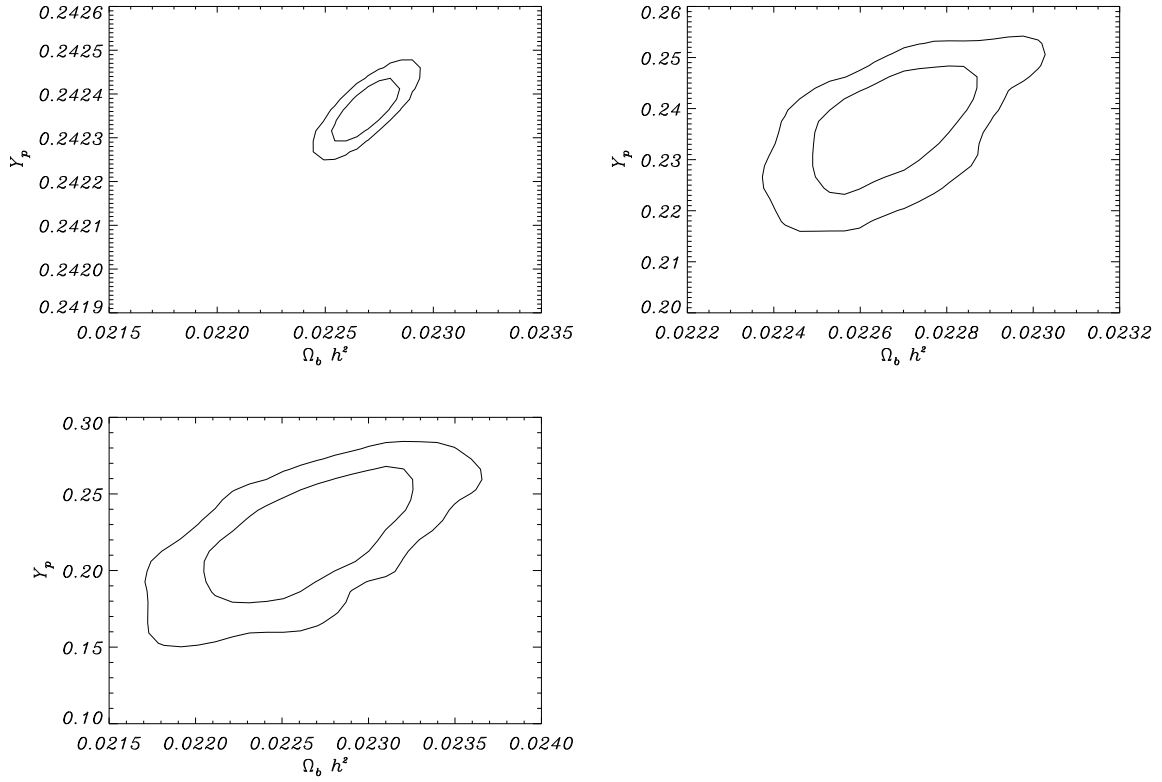


Figure 11: The $Y_p - \Omega_b h^2$ degeneracy: Shown are results for PLANCK with $\xi_\nu = 0$ (top left), PLANCK with $\xi_\nu \neq 0$ (top right), and POLARBEAR with $\xi_\nu \neq 0$ (bottom). The fiducial cosmological model is as described in Fig. 5.